Effects of Mineral Crystal Structure And Properties On The Macro-Mechanical Properties of Rocks

Yongyan Yan
Zhengzhou University
Wuxiu Ding (wuxiu-ding@163.com)
Luoyang Institute of Science and Technology https://orcid.org/0000-0002-0435-2623
Guoji Liu
Zhengzhou University
Hongyi Wang
Luoyang Institute of Science and Technology

Research Article

Keywords: crystal structure, chemical bond, First Principle, elastic modulus, calcite, dolomite

Posted Date: January 21st, 2022

DOI: https://doi.org/10.21203/rs.3.rs-1207534/v1

Abstract

Rock is a nonhomogeneous material composed of one or more minerals. The structure and properties of internal mineral crystals have an impact on its macro-mechanical properties. Taking the Longmen Grottoes limestone as the research object, firstly, the mineral composition and macro-mechanical properties of the limestone are obtained, and through simulation and calculation of the crystal structure, chemical bond properties and elastic properties of minerals, this paper reveals how the mineral crystal structure and properties affect the macro-mechanical properties of the rock. Tests show that the main mineral components of the limestone in Longmen Grottoes are calcite and dolomite crystals. The uniaxial compression strength and elastic modulus of limestone with different calcite and dolomite contents are obviously different. From the study of crystal structure and chemical bond properties, it is learnt that the calcite and dolomite have similar crystal structures, but due to the difference of the chemical bond strength of Ca-O and Mg-O, the overall calcite crystal has a weaker chemical bond strength than the whole dolomite crystal. The First Principle simulation suggests a correlation between the overall crystal chemical bond strength and elastic modulus of the crystal. Therefore, studying the crystal structure and properties of minerals provides a significant research direction for revealing the mechanism of the macro-mechanical properties of rocks.

1. Introduction

Rock is a nonhomogeneous material composed of one or more minerals. The macro-mechanical properties of the rocks are closely related to the internal mineral structures and properties. Determining the qualitative and quantitative relationship between rock macro-mechanical properties and mineral crystal structure and properties remains to be a challenge in rock mechanics research.

Scholars have long recognized the influence of mineral composition on the mechanical properties of rocks and have carried out related research. Bin et al. (2013) studied 9 different rock samples (including magmatic rock, chemical sedimentary rock and clastic sedimentary rock), and analyzed the qualitative relationship between mineral composition, micro-structure and mechanical property parameters. It is found that feldspar minerals are the main cause of rock brittleness. The higher content of calcite in granite makes its compressive strength and elastic modulus smaller. The content of quartz in granite is higher and its cohesive force is higher. For clay rocks, the content of clay minerals weakens the mechanical properties of the rock. For the example of red sandstone, the uniaxial compressive strength decreases with the increase of clay mineral content (Zhihong et al. 2010) while the Poisson's ratio decreases with the decrease of clastic feldspar and quartz particles (Huamin et al. 2018). Gray-green and red mudstones are mainly powdery clay particles, but the gray-green mudstone has more clay mineral content, more uniform particle size distribution, and better gradation, so the shear strength of gray-green mudstone is better than red mudstone (Wenwu et al. 2016). By comparing the relationship between the mineral content, particle size and uniaxial compressive strength of granite samples (Guangxiang et al. 2018), it is found that the minerals that have the greatest impact on the uniaxial compressive strength of granite are potassium feldspar and biotite, while plagioclase and quartz have little impact. The

correlation between mineral particle size and uniaxial compressive strength is not obvious. The above results are mainly concerned with the qualitative study of mineral composition and content on the mechanical properties of rocks. There are few reports about the effects of mineral crystal structure and properties on the macro-mechanical properties of rocks.

Minerals have a relatively stable internal structure and chemical composition. Most solid minerals are crystalline minerals, which can be studied with crystal chemistry method. Chemical bond refers to the strong interaction between adjacent atoms or ions. The calculation of chemical bond is vital for understanding the microscopic properties of mineral crystals (Zhaohua et al.2011). Shuoshi et al. (2008) calculated the chemical bond properties of the crystal structure of sulfate minerals, which provide a theoretical basis for studying the minerals floatability and the crystal structure. The more advanced computer simulations tackle the difficulty in crystal microscopic tests, so the microscopic properties of mineral crystals can be further studied.

The molecular simulation technology can simulate the adsorption of mineral crystals and water molecules (Jianhua, et al. 2017; Peng et al. 2017) or gas molecules (Shuangfang et al. 2018), and solve the problems of rock gas storage and mineral flotation through the calculation of adsorption energy. Tao et al. (2017) used molecular dynamics simulation technology to study the effects of temperature and pressure on the volume, density, Young's modulus and Poisson's ratio of the main mineral crystals in granite. However, these experiments failed to connect the crystal structure and properties of minerals with the macro-mechanical properties of rocks.

This paper takes the limestone in the Longmen Grottoes area as the research object. In the first place, the mineral composition of the rock is obtained through X-ray diffraction test, and the uniaxial compression test is conducted to obtain the uniaxial compressive strength and elastic modulus of the limestone. Further, the crystal structure of the main mineral crystals of limestone is studied, and the chemical bond properties and elastic properties of the crystals are calculated with application of chemical formulas and First Principle. Finally, the effects of mineral crystal structure and properties on the macro-mechanical properties of rock is analyzed, and the causes of the difference in macro-mechanical properties of limestone with different mineral content are explained.

2. Materials And Methods

2.1 Sample Preparation

The limestone for this experiment was taken from the Longmen Mountain, Luoyang, China, where the Longmen Grottoes located, as shown in Fig. 1. In this area, the limestone mineral composition is simple, the limestone has excellent mechanical strength and deformation resistance. The test selected intact rock blocks with no obvious defects, and during transportation and processing, collisions were reduced and mechanical damage to the rock was avoided. According to the national standards of "Engineering Rock Mass Test Method Standard" (GB/T 50266-2013), a cylindrical standard specimen with a diameter of 50mm and a height of 100mm is prepared through drilling and coring processes.

2.2 X-ray Diffraction Test Results

X-ray diffraction test was done on the sample with the X-ray diffractometer (X'Pert PRO, produced by PANalytical, Netherlands) to obtain the diffraction pattern of the limestone sample, and the X-ray diffraction data was analyzed by the MDI JADE software to obtain the specific mineral composition and content in it. Then the limestone samples are divided into four categories according to the mineral content, which are numbered $A^{\#}$, $B^{\#}$, $C^{\#}$ and $D^{\#}$. The X-ray diffraction pattern of the limestone sample is shown in Fig. 2, and the mineral composition and content are shown in Table 1.

Table 1 Mineral composition and content of limestone sample

No.	Calcite /%	Dolomite /%	Others /%
$A^{\#}$	60.9	37.2	1.9
$B^{\#}$	75.1	22.6	2.3
$C^{\#}$	76.6	21.0	2.4
$D^{\#}$	79.2	18.4	2.4

By comparing the data sourced from the International Center for Diffraction Data (ICDD), it is learnt that the main mineral components of the limestone in the Longmen Grottoes are calcite and dolomite crystals. Through the quantitative analysis of MDI JADE software, the content of calcite and dolomite in the limestone samples range from 60.9%-79.2% and 18.4%-37.2% respectively, and other components were within 2.4%.

2.3 Uniaxial Compression Test Results

The uniaxial compression test was conducted on four kinds of limestone samples with different mineral contents, and the stress-strain curve and compressive strength of the samples were obtained, as shown in Fig. 3. Meanwhile, the elastic modulus of limestone is calculated, and the mechanical parameters are shown in Table 2. The equipment used is a rock and concrete mechanics test system (RMT-301) which is independently developed by the Wuhan Institute of Rock and Soil Mechanics, Chinese Academy of Sciences. It meets the national standards and can meet the needs of engineering applications and basic theoretical research.

Table 2 Mechanical parameters of different mineral contents

No.	Compressive strength /MPa	Elastic Modulus /GPa
A#	142.47	61.41
B#	124.80	54.35
C#	106.57	50.79
D#	95.55	44.51

Since the four limestone samples selected have no obvious cementation components, this paper only considers the effects of the main mineral contents of limestone (calcite and dolomite crystals) on the macro-mechanical properties of limestone. Figure 3 indicates that the limestone presents four stages: compaction stage, linear elastic stage, yield stage, and failure stage. During the compaction stage, the stress-strain curve goes upwards, which is related to the contact between the particles in the rock. The existence of microscopic defects such as pores and micro-cracks between the rock particles makes the rock present nonlinear characteristics at the initial stage of compaction. As the load increases, the spaces between the mineral particles are compacted. In the elastic stage, the stress-strain curve presents a linear correlation. As the content of calcite increases (the content of dolomite decreases), the elastic modulus of limestone gradually decreases, and its elastic modulus varies from 44.51 to 61.41 GPa. In the yield stage, the stress-strain curve deviates from the linear correlation, and imperceptible cracks are gradually formed in the rock under the load. When it reaches the ultimate load, the rock is quickly destroyed. As the content of calcite increases (the content of dolomite decreases), the peak strength of limestone gradually decreases, and its variation range is 95.55~142.47MPa. In the failure stage, the stress of the four kinds all showed a vertiginous decline, indicating the brittleness of the limestone. Table 2 suggests that along with the decrease of calcite and the increase of dolomite, the compressive strength and elastic modulus of limestone are getting higher.

3 Research On Mineral Crystal Structure And Microscopic Properties

The uniaxial compression test results show that the uniaxial compressive strength and elastic modulus of limestone are closely related to calcite and dolomite. To better understand the microscopic causes for the difference in the macro-mechanical properties of limestone, the crystal structure, chemical bond properties and elastic properties of calcite and dolomite were studied.

3.1 Mineral Crystal Structure

The molecular formula of calcite is $CaCO_3$, which is a traigonal crystal, and the spatial structure is R□3c. The hexagonal unit cell is used for simulation calculation. The unit cell parameters are a=b=0.4988nm, c=1.7061nm, α = β = 90°, γ = 120°, Z=6 (Guoshan 2010). The molecular formula of dolomite is $CaMg(CO_3)_2$. The structure is similar to the calcite, and it is also a trigonal crystal, the spatial structure is R 3, the hexagonal unit cell parameters are a=b=0.4808nm, c=1.601nm, α = β = 90°, γ = 120°, Z=3. The

crystal structure of dolomite can be regarded as half of the Ca^{2+} in the calcite structure is completely replaced by Mg^{2+} and is sequential. Since the ionic radius of Mg^{2+} is smaller than that of Ca^{2+}, the unit cell parameters of dolomite are smaller than that of calcite. The crystal structures of calcite and dolomite are shown in Fig. 4.

3.2 Crystal Chemical Bond Properties

The strength of the chemical bond between anion and cation in the crystal structure determines the mineral cleavage. The calculation and analysis of the chemical bond properties in the crystal structure of calcite and dolomite are of great significance for predicting the macro-mechanical properties of limestone.

3.2.1 Calculation and Results of Crystal Chemical Bonds

The M^{n+}-X^{n-} bonds in calcite crystals include Ca-O bonds and C-O bonds, and the M^{n+}-X^{n-} bonds in dolomite crystals include Ca-O bonds, Mg-O bonds and C-O bonds, in which M^{n+} represents metal cations and X^{n-} represents anion. According to the crystal chemical formula and crystal parameters, the ionic electrostatic valence strength, ionic bond percentage, Coulomb force, ionic bond polarity and average bond valence of calcite and dolomite crystals can be calculated. The ionic electrostatic valence strength refers to the strength of the bond between the cation and anion (Meichen 1993). Ionic bond percentage and ionic bond polarity refer to the ionicity of chemical bonds in a compound, and the larger the value, the easier it is to break. Coulomb force refers to the electrostatic attraction between anion and cation. Average bond valence is an expression of the strength of chemical bonds in bond valence theory. It is believed that a chemical bond composed of specific atoms has a larger bond length value. When the bond value gets smaller, the bond strength becomes weaker, and vice versa (Brown and Shannon 1973). The chemical bond parameters, calculation formulas and results are shown in Table 3.

Table 3

Calculations and results of M^{n+}-X^{n-} bonds in calcite and dolomite crystals

Chemical bond Mineral	**Calcite**		**Dolomite**		
Parameters and calculation formula					
M^{n+}-X^{n-} Bonds	Ca-O	C-O	Ca-O	Mg-O	C-O
M Cation Electrovalence Z	2	4	2	2	4
M Cation Radius Rc/nm	0.099	0.015	0.099	0.072	0.015
M Coordination Number CN	6	3	6	6	3
M Element Electronegativity	1	2.55	1	1.31	2.55
Electrostatic Valence Intensity $S=\frac{Z}{CN}$	1/3	4/3	1/3	1/3	4/3
M^{n+}-X^{n-} Bond Length R/ Å	2.51	1.56	2.47	2.03	1.50
M^{n+}-X^{n-} Ionic Bond Percentage $\phi = 100\left[1 - e^{-\left(X_A - X_B\right)^2/4}\right]/\%$	77.43	17.97	77.43	67.83	17.97
M^{n+}-X^{n-} Coulomb Force $F_{k=}K\frac{Z_M Z_X e^2}{\left(R_c + R_a\right)}/(*10^{-8}N)$	1.613	7.672	1.613	2.051	7.672
M^{n+}-X^{n-} Bond Polarity $\lambda=\frac{F_X - F_M}{F_X + F_M}$	0.70	-	0.70	0. 55	-
M^{n+}-X^{n-} Average Bond Valence $S'=\left(\frac{R}{R_0}\right)^{-N} or S' = e^{-\left(\frac{R-R_0}{B}\right)}$	0.224	0.540	0.247	0.385	0.681

Remarks

X_A and X_B are the electronegativity of two kinds of atoms, F_X is the bond force of non-metal ions, F_M is the bond force of metal ions, $F_{X/M}$, rc is the ion covalent radius, O ion radius Ra=0.140nm, O Electronegativity X_O=3.44nm, e=1.6*10^{-19}C, ion covalent radius r_{Ca}=0.174nm, r_{Mg} =0.136nm, r_O =0.073.

3.2.2 Analysis of Chemical Bond Properties

Table 3 indicates the rules between the bond length, ionic bond percentage, Coulomb force, ionic bond polarity and average bond valence of the crystal: the shorter the M^{n+}-X^{n-} bond length, the smaller the bond polarity, and the larger the average bond valence, the larger the Coulomb force, the M^{n+}-X^{n-} bond is harder to break. Due to the similar crystal structures of calcite and dolomite, the Ca-O bond in calcite and the Ca-O bond in dolomite have the same electrostatic valence strength, ionic bond percentage, Coulomb force, and ionic bond polarity. However, the Ca-O bond of dolomite is slightly shorter than that of calcite, which causes the average bond value of the Ca-O bond of dolomite to be slightly larger than that of calcite, but the difference is very small, so the properties of Ca-O in the two crystals are discussed together. The C-O bond is taken in the same way. Comparing Ca-O and Mg-O bond with C-O bond, the bond lengths of Ca-O and Mg-O are larger, the electrostatic valence strength, Coulomb force and average bond valence are lower, while the ionic bond percentage and the ionic bond polarity are larger, indicating that the bond strengths of Ca-O and Mg-O are obviously weaker than the C-O bond, so the Ca-O and Mg-O bonds are easier to break comparing to C-O bond. For Ca-O and Mg-O bond, the bond length of Ca-O is longer than that of the Mg-O bond, the Coulomb force and the average bond valence are smaller than that of the Mg-O bond, and the ionic bond percentage and polarity of the Ca-O bond are larger than that of Mg-O bond, this indicates that the Ca-O bond is weaker than the Mg-O bond and Ca-O bond is easier to break.

The crystal structures of dolomite and calcite is similar. The dolomite crystals can be considered as calcite crystals with half of the Ca^{2+} replaced by Mg^{2+}. The bond length of the Mg-O is shorter than that of Ca-O bond. The calculation of the chemical bond shows that the strength of the Mg-O bond is greater than that of the Ca-O bond. The strength of all Ca-O bonds in dolomite crystals is roughly equal to the strength of half of the Ca-O bonds in calcite crystals, and the strength of all Mg-O bonds is greater than the strength of the other half of Ca-O bonds in calcite crystals, which means the overall chemical bond strength of dolomite crystals is greater than its counterpart of calcite crystals.

3.3 Crystal Elastic Properties

The elastic constant of the crystal reflects the degree of crystal's response to external forces, and is an important parameter that determines the elastic properties of the material. In this paper, the First Principle method based on density functional theory is used to study the elastic properties of mineral crystals.

3.3.1 Simulation Process and Geometric Optimization

The calculation uses Materials Studio software. Input the unit cell parameters to establish the crystal parameters of calcite and dolomite, build the model shown in Fig. 3, and then select the CASTEP module for geometric optimization. The parameters are as follows: select Geometric Optimization in the Task, select Fine for the calculation accuracy, the system energy converges to1.0×10^{-5}eV/atom, the average atomic force converges to 0.03 eV/nm, the tolerance deviation converges to 0.001 Å, and the stress deviation converge to 0.05 GPa, select BFGS algorithm. In addition, the exchange correlation function, cutoff energy, and K point parameter selection are tested, and the results are shown in Fig. 5.

The lattice parameters and energy of calcite and dolomite will change along with the simulation parameters. Thermodynamics shows that when the total energy is the smallest, the crystal structure is the most stable. According to the calculation, the calcite and dolomite are selected for geometric optimization under the conditions of exchange correlation function GGA/PW91, cutoff energy of 380eV, K point 3×3×1, and the optimized calcite lattice parameters are: a=b=5.05229 Å, c=17.2129 Å, the dolomite lattice parameters are: a=b=4.87871 Å, c=16.2701 Å.

3.3.2 Simulation Results and Analysis of Crystal Elastic Properties

The elastic constants and other elastic properties of crystals can give us a deeper understanding of the micro-mechanical properties of mineral crystals. The molecular simulation technology to calculate the elastic parameters of the crystal is based on the "stress-strain" method, that is, the elastic constant of the crystal is obtained by the stress change caused by the different strains. For trigonal crystals, such as calcite and dolomite, the "stress-strain" relationship can be expressed in matrix form, as shown in Eq. (1).

$$\begin{pmatrix} \sigma_{11} \\ \sigma_{22} \\ \sigma_{33} \\ \sigma_{23} \\ \sigma_{31} \\ \sigma_{12} \end{pmatrix} = \begin{pmatrix} C_{11} & C_{12} & C_{13} & C_{14} & & \\ C_{12} & C_{11} & C_{13} & -C_{14} & & \\ C_{13} & C_{13} & C_{33} & & & \\ C_{14} & -C_{14} & & C_{44} & & \\ & & & & C_{44} & C_{14} \\ & & & & C_{14} & \frac{C_{11}-C_{12}}{2} \end{pmatrix} \begin{pmatrix} e_{11} \\ e_{22} \\ e_{33} \\ e_{23} \\ e_{31} \\ e_{12} \end{pmatrix} \quad (1)$$

Materials Studio software is used to calculate the elastic constants of optimized calcite and dolomite crystals. To calculate all the elastic constants, the crystal structure needs to be optimized in six strain modes, and the maximum strain is set to 0.003. To improve the precision of elastic constants, the total energy convergence standard is increased to 2.0×10-6e V/atom. Other convergence standards and K point settings are consistent with the previous geometric optimization. Calculate the elastic modulus C_{11}, C_{12}, C_{13}, C_{14}, C_{33} and C_{44} of calcite and dolomite. According to the elastic constant of the crystal, the Voigt-Reuss-Hill theory (Hill 1952; Pham 2003) can be applied to further calculate the crystal elastic properties of calcite and dolomite. Among them, the calculation formulas for the bulk modulus, shear modulus and Young's (elastic) modulus of the trigonal crystal are shown in Eq. (2).

$$B_V = \frac{1}{9}\left(2C_{11} + 2C_{12} + 4C_{13} + C_{33}\right)$$

$$G_V = \frac{1}{30}\left(7C_{11} - 5C_{12} - 4C_{13} + 2C_{33} + 12C_{44}\right)$$

$$B_R = \frac{\left(C_{11} + 2C_{12}\right)C_{33} - 2C_{13}^2}{C_{11} + C_{12} - 4C_{13} + 2C_{33}}$$

$$G_R = \frac{15}{2}\left[\frac{2C_{11} + 2C_{12} + 4C_{13} + C_{33}}{C_{33}\left(C_{11} + C_{12}\right) - 2C_{13}^2} + \frac{3C_{11} - 3C_{12} + 6C_{44}}{C_{44}\left(C_{11} - C_{12}\right) - 2C_{14}^2}\right]$$

$$B = \frac{1}{2}\left(B_V + B_R\right)$$

$$G = \frac{1}{2}\left(G_V + G_R\right)$$

$$E = \frac{9BG}{3B + G}$$

2

The elastic parameters of calcite and dolomite crystals are shown in Table 4 and Table 5.

Table 4
Elastic parameters of calcite crystal (unit: GPa)

elastic parameters	present work	calculated		experiment	
		Junhua (2009)	Ayoub (2011)	Hearmon(1979)	Chienchih (2001)
C_{11}	147.20	146.82	152.3	144.0	149.4
C_{12}	23.68	47.87	57.05	53.9	57.9
C_{13}	53.29	46.05	54.83	51.1	53.5
C_{14}	15.54	-16.81	17.14	-20.5	-20.2
C_{33}	85.16	91.76	87.77	84.0	85.2
C_{44}	38.3	32.52	36.00	33.5	34.1
B	70.20				
G	39.74				
E	100.29				

Table 5
Elasticity parameters of dolomite crystal (unit: GPa)

elastic parameters	present work	calculated		experiment	
		Titiloye(1998)	Bakri(2011)	Humbert (1972)	Pofei (2006)
C_{11}	200.97	201.6	196.6	205	204.1
C_{12}	33.23	68.4	64.4	71	68.5
C_{13}	53.38	58.2	54.71	57.4	45.8
C_{14}	14.05	10.7	22.45	-19.5	20.6
C_{33}	106.55	105.4	110.01	112.8	97.4
C_{44}	43.62	41.7	41.57	39.8	39.1
B	84.98				
G	53.88				
E	133.44				

According to the lattice dynamics theory (Born 1955), the elastic constant C_{ij} of the crystal needs to meet the mechanical stability, and the conditions of the structural stability of the trigonal crystal is shown in Eq. (3).

$$C_{11} - \left|C_{12}\right| > 0$$

$$\left(C_{11} + C_{12}\right)C_{33} - 2C_{13}^2 > 0$$

$$\left(C_{11} - C_{12}\right)C_{44} - 2C_{14}^2 > 0$$

3

Substituting the calculated elastic constants of calcite and dolomite crystals into Eq. (3), the calculation results meet the conditions, indicating that the calculated elastic constants C_{ij} of calcite and dolomite crystals meet the structural stability standard, that is, it is feasible to calculate the elastic constants of crystals with application of First Principle.

Normally, the elastic constants C_{11} and C_{33} indicate the resistance of the material to the strain along the axial-axis and the radial-axes (Hadi 2019). When C_{11}>C_{33}, the compressibility along the axial-axis is weaker than the radial-axes, otherwise the opposite. It can be seen from Table 4 and Table 5 that both calcite and dolomite have relatively weak compressibility along the axial-axis. The difference in value

between C_{12} and C_{44} (C_{12}-C_{44}) is defined as the Cauchy pressure, which can be used to differentiate the brittleness and ductility of the material. If the Cauchy pressure value is positive, the material is ductile, otherwise the material is brittle (Du 2008). Table 4 and Table 5 show Cauchy pressures of calcite and dolomite crystals are 8.14GPa and 19.18GPa, indicating that both calcite and dolomite crystals are brittle. The calculation shows that the bulk modulus, shear modulus, and elastic modulus of dolomite are greater than that of calcite, and because the overall chemical bond strength of dolomite crystal is greater than that of calcite, we speculate that there is a correlation between the overall chemical bond strength and the elastic modulus of the crystal. The stronger the chemical bond strength of the crystal, the greater the elastic modulus of it.

4 Conclusion

To conclude, we found that the structures and properties of calcite and dolomite crystals are of great importance to the macro-mechanical properties of the limestone in Longmen Grottoes. Both calcite and dolomite are trigonal crystals, despite their similar structures, the bond strength of the Ca-O is weaker than that of the Mg-O, making the overall chemical bond strength of the calcite crystal weaker than that of the dolomite crystal. We found that there is a correlation between the overall chemical bond strength and the elastic modulus of the crystal. The stronger the overall chemical bond strength of the crystal, the greater the elastic modulus. Due to the difference in the crystal structures and properties of calcite and dolomite, the uniaxial compressive strength and elastic modulus of limestones with different contents of calcite and dolomite are different. Therefore, the crystal structures and properties of minerals are one of the main causes that affect the macro-mechanical properties of limestones with different mineral contents.

The connection of the macro-mechanical properties of rocks, the crystal structures and properties of minerals is rather complicated. In further research, we plan to take rock cracks and crystal structure defects into consideration.

Declarations

Acknowledgments: The author thanks Zhengzhou University and Luoyang Institute of Technology for the experimental instruments and simulation software provided.

Funding: The work presented in this paper is financially supported by the National Natural Science Foundation of China (Grant Nos. 51279073).

Data Availability Statement: The data presented in this study are available on request from the

corresponding authors.

Conflict of interest The authors declare no confict of interest.

References

1. Bin Z, Zhiyin W, Jinpeng W (2013) Relation between mineralogical composition and microstructure to the mechanical properties of rock materials. Coal Geology & Exploration 41(03):59–6367
2. Zhihong L, Wei X, Yunming Z (2010) Experimental research on influences of physical indices and microstructure perameters on strength properties of red stone from Western Hunan. Chin J Rock Mechan Eng 29(01):124–133
3. Huamin L, Huigui L, Kailin W, Chuang L (2018) Effect of rock composition microstructure and pore characteristics on its rock mechanics properties. International Journal of Mining Science and Technology 28(02):303–308. https://doi.org/10.1016/j.ijmst.2017.12.008
4. Wenwu C, Gaochao L, Wei L et al (2016) Physical and mechanical properties of weathered green and red mudstones. Chin J Rock Mechan Eng 35(12):2572–2582. .https://doi.org/10.13722/j.cnki.jrme.2016.0822
5. Guangxiang Y, Luqing Z, Qingli Z et al (2018) Correlation of the mineralogical characteristics with the uniaxial compressive strength of granite. Hydrogeology & Engineering Geology 45(05):93–100. https://doi.org/10.16030/j.cnki.issn.1000-3665.2018.05.13
6. Zhaohua S, Erfeng R, Kai L (2011) Application of bond price theory in minerals. Acta Mineralogica Sinica 31(S1):548–549
7. Shuoshi L, Chuanyao S (2008) Theoretical Calculation on Chemical Bond of Some Sulfate Minerals Crystal Structure. Nonferrous Wetals 02:104–106. https://doi.org/10.3969/j.issn.2095-1744.2008.02.025
8. Jianhua C, Ye C, Xianhao L, Yuqiong L (2017) DFT study of coadsorption of water and oxygen on galena (PbS) surface: An insight into the oxidation mechanism of galena. Appl Surf Sci 420:714–719. .https://doi.org/10.1016/j.apsusc.2017.05.199
9. Peng X, Wenli L, Zongyi Y, Jun C (2017) Influence of carbon atom adsorption on coal pyrite hydrophobicity based on quantum chemistry. Journal of China Coal Society 42(05):1290–1296. https://doi.org/10.13225/j.cnki.jccs.2016.1005
10. Shuangfang L, Bojian S, Chenxi X et al (2018) Study on adsorption behavior and mechanism of shale gas by using GCMC molecular simulation. Earth Sci 43(05):425–433. https://doi.org/10.3799/dqkx.2018.430
11. Tao C, Jinming X (2017) Effects of temperature and pressure on microscopic physical and mechanical features of minerals in granite. Journal of Engineering Geology 25(06):1474–1481. .https://doi.org/10.13544/j.cnki.jeg.2017.06.010
12. Guoshan C (2010) Fundamentals of Mineralogy. Metallurgical Industry Press
13. Meichen S (1993) Pauling's rule and the Bond Valence Theory. Higher Education Press
14. Brown ID, Shannon RD (1973) Empirical bond-strength–bond-length curves for oxides. Acta Cryst 29(3):266–282. https://doi.org/10.1107/S0567739473000689

15. Hill R (1952) *The Elastic Behaviour of a Crystalline Aggregate.* Proceedings of the Physical Society. Section A **65**(5): p. 349-354. https://doi.org/10.1088/0370-1298/65/5/307
16. Pham DC (2003) Asymptotic estimates on uncertainty of the elastic moduli of completely random trigonal polycrystals. Int J Solids Struct 40(18):4911–4924. https://doi.org/10.1016/S0020-7683(03)00141-0
17. Junhua Z, Bin Z, Baiguo L, Wanlin G (2009) Elasticity of Single-Crystal Calcite by First-Principles Calculations. J Comput Theor Nanosci 6(5):1181–1188. https://doi.org/10.1166/jctn.2009.1163
18. Ayoub A, Zaoui A, Berghout A (2011) High-pressure structural phase transitions and mechanical properties of calcite rock. Comput Mater Sci 50(3):852–857. https://doi.org/10.1016/j.commatsci.2010.10.021
19. Hearmon RFS (1979) The elastic constants of crystals and other anisotropic materials; the third- and higher-order elastic constants. Landolt-Börnstein: Numerical Data and Functional Relationships in Science and Technology 11:245–286
20. Chienchih C, Chungcherng C, Lingun L et al (2001) Elasticity of single-crystal calcite and rhodochrosite by Brillouin spectroscopy. Am Mineral 86(11–12):1525–1529. https://doi.org/10.2138/am-2001-11-1222
21. Titiloye JO, Leeuw NHde, Parker SC (1998) Atomistic simulation of the differences between calcite and dolomite surfaces. Geochim Cosmochim Acta 62(15):2637–2641. https://doi.org/10.1016/S0016-7037(98)00177-X
22. Bakri Z, Zaoui A (2011) Structural and mechanical properties of dolomite rock under high pressure conditions: A first-principles study. physica status solidi (b) 248(8):1894–1900. https://doi.org/10.1002/pssb.201046465
23. Humbert P, Plicque F (1972) *Propriétés élastiques de carbonates rhomboédriques monocristallins: Calcite, magnésite, dolomite.* Comptes Rendus de l'Académie des Sciences de Paris **275**: p. 391-394
24. Pofei C, Lingyun C, Paohsien H et al (2006) Elasticity of magnesite and dolomite from a genetic algorithm for inverting Brillouin spectroscopy measurements. Physics of the Earth & Planetary Interior 155(1–2):73–86. https://doi.org/10.1016/j.pepi.2005.10.004
25. Born M (1955) The Dynamic Theory of Crystal Lattices. Am J Phys 23(7). https://doi.org/10.1119/1.1934059
26. Hadi MA, Kelaidis N, Naqib SH et al (2019) *Mechanical behaviors, lattice thermal conductivity and vibrational properties of a new MAX phase Lu2SnC*. 129:: p. 162–171. https://doi.org/10.1016/j.jpcs.2019.01.009
27. Du YL, Sun ZM, Hashimoto H, Tian WB (2008) *First-Principles Study of Carbon Vacancy in Ta4AlC3*. 49:1934–1936. https://doi.org/10.2320/matertrans.MAW200803. 9): p.

Figures

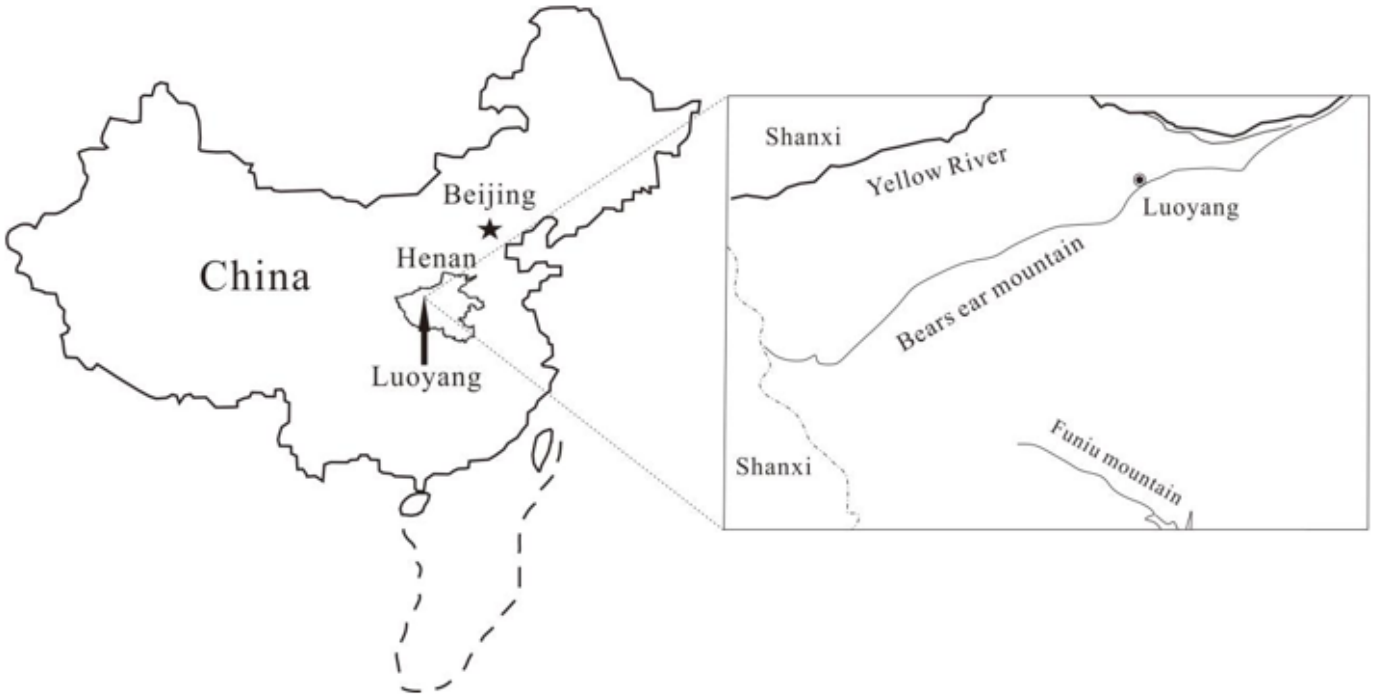

Figure 1

Map of the study area

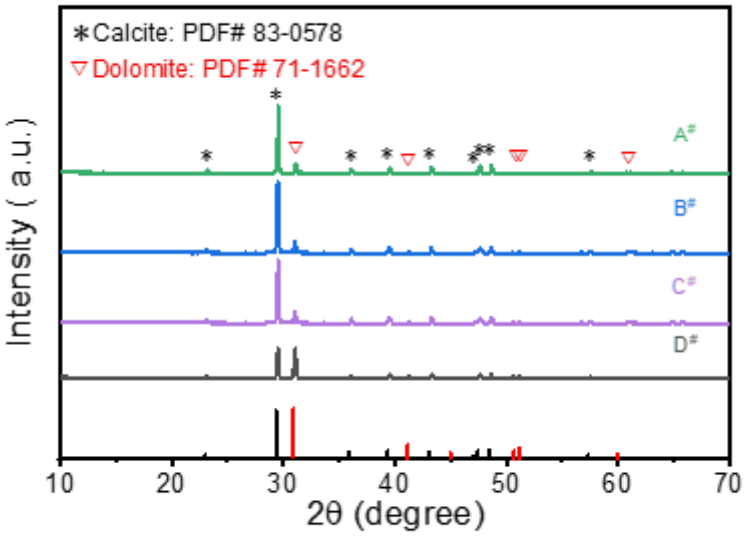

Figure 2

X-ray diffraction pattern of limestone sample

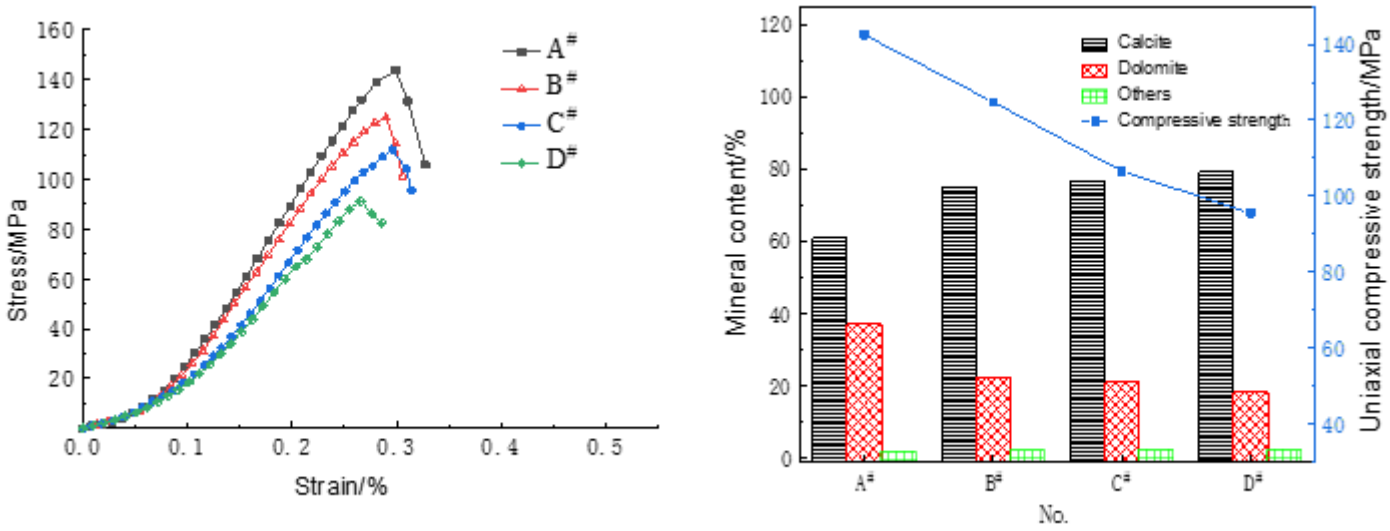

Figure 3

Uniaxial compression stress-strain curve and compressive strength of limestone samples

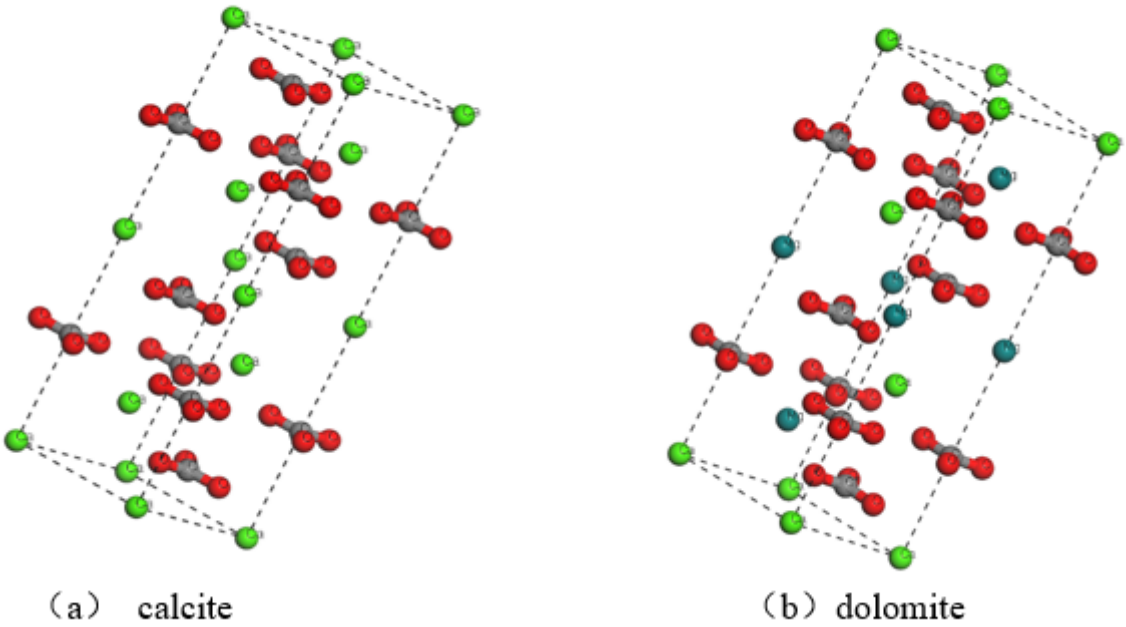

Figure 4

Calcite and dolomite

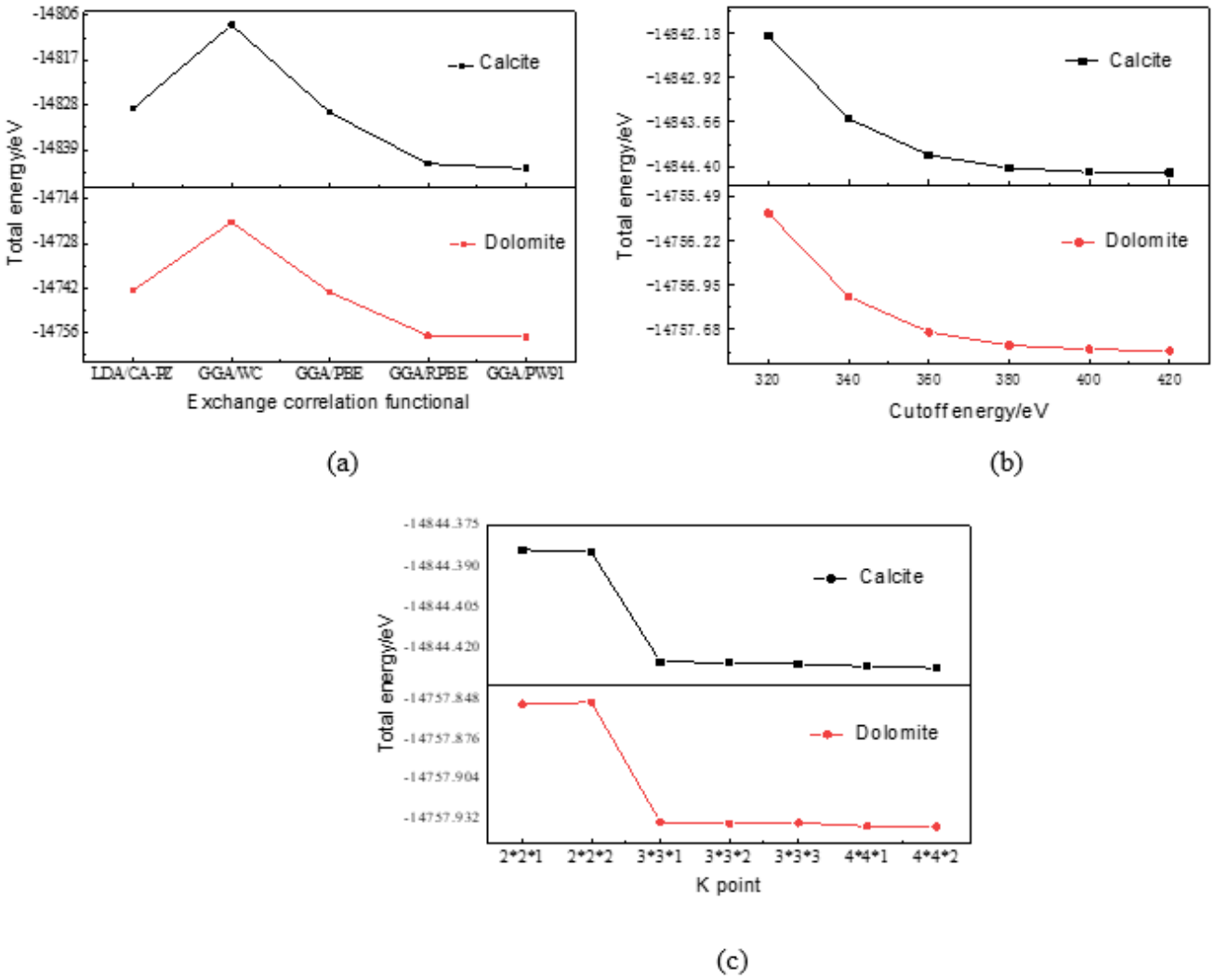

Figure 5

Calcite and dolomite geometric optimization conditions are determined:

Figrue a is the total energy of the crystal when the exchange correlation functional changes (cutoff energy and K point are default).

Figrue b is the total energy of the crystal when the cutoff energy changes (exchange correlation function is GGA/PW91, K point is default).

Figrue c is the total energy of the crystal when the K point changes (the exchange correlation function is GGA/PW91, and the cutoff energy is 380eV).